矿物岩石地球化学通报
Bulletin of Mineralogy, Petrology and Geochemistry
Vol.43 No.6, Nov., 2024

深俯冲洋壳脱碳作用与榴辉岩型深源金刚石成因：进展与挑战

张艳飞[1],王超[1],章军锋[2*],巫翔[1],朱峰[2]

1. 中国地质大学(武汉）地质过程与矿产资源国家重点实验室,武汉 430074;
2. 中国地质大学(武汉）地球科学学院,武汉 430074

摘　要：蚀变洋壳是俯冲带碳输运的主要寄主岩石之一,具有把大量碳输运至地球内部和促进地幔碳循环的潜力。金刚石是直接来自地幔深部的单质碳,包含了地幔深部有关碳赋存和碳迁移的重要信息。高温高压实验是研究俯冲洋壳脱碳过程的正演模拟手段,而榴辉岩型深源金刚石则直接指示了俯冲洋壳在地幔深部的脱碳过程,二者相互结合能较完整地刻画深俯冲洋壳的脱碳机制和碳迁移过程。本文综述了前人有关榴辉岩型深源金刚石来源深度和俯冲含碳洋壳高温高压实验岩石学研究方面的进展,对比讨论了榴辉岩型深源金刚石的成因,最后提出了几点值得进一步研究的方向。

关　键　词：俯冲洋壳;脱碳作用;深源金刚石;下地幔

中图分类号：P542.5　**文章编号：**1007-2802(2024)06-1160-11　**doi:** 10.3724/j.issn.1007-2802.20240121

The decarbonization of deeply subducted oceanic crusts and genesis of super-deep eclogitic diamonds: progresses and challenges

ZHANG Yan-fei[1], WANG Chao[1], ZHANG Jun-feng[2*], WU Xiang[1], ZHU Feng[2]

1. *State Key Laboratory of Geological Processes and Mineral Resources, School of Earth Sciences, China University of Geosciences (Wuhan), Wuhan* 430074*, China;*
2. *School of Earth Sciences, China University of Geosciences(Wuhan), Wuhan* 430074*, China*

Abstract: Altered basalt of oceanic crust is one of the main host rocks for the transportation of carbon in subduction zones, I has the potential to transport significant amounts of carbon into the Earth's interior and to promote the cycling of carbon in the mantle. Diamond is a simple carbon directly sourced from the deep part of the mantle. It contains important information about the storage and migration processes of carbon in the deep part of the mantle. The high-pressure and high-temperature experiment is used as a forward modeling method to study the decarbonization process of the subducted oceanic crust. Eclogitic diamonds directly reflect the decarbonization process of subducted oceanic crust in the deep part of the mantle. The combination of these two methods can be used to completely characterize the decarbonization mechanism and carbon migration process of the deeply subducted oceanic crust. In this paper, we have summarized progresses of researches on the depth of deeply sourced ecologitic diamonds and progresses of the high-pressure and high-temperature experimental petrological studies on the subducted carbon-bearing oceanic crusts, discussed the genesis of eclogitic diamonds based on the comparative study, and finally proposed several directions worth for the further research.

收稿编号:2024-0138,2024-7-24 收到,2024-9-11 改回
基金项目:国家重点研发计划(2023YFF0804100);国家自然科学基金面上项目(42372068)
第一作者简介:张艳飞(1986—),男,研究员,博士生导师,研究方向:实验岩石学. E-mail:yanfzhang@cug.edu.cn.
*通信作者简介:章军锋(1977—),男,教授,博士生导师,研究方向:构造物理学. E-mail:jfzhang@cug.edu.cn.

引用此文:
张艳飞,王超,章军锋,巫翔,朱峰. 2024. 深俯冲洋壳脱碳作用与榴辉岩型深源金刚石成因:进展与挑战. 矿物岩石地球化学通报,43(6):1160–1170. doi: 10.3724/j.issn.1007-2802.20240121
Zhang Y F,Wang C,Zhang J F,Wu X,Zhu F. 2024. The decarbonization of deeply subducted oceanic crusts and genesis of super-deep eclogitic diamonds: progresses and challenges. Bulletin of Mineralogy, Petrology and Geochemistry,43(6):1160–1170. doi: 10.3724/j.issn.1007-2802.20240121

Key words: subducted oceanic crust; decarbonization; super-deep diamond; lower mantle

0　前言

俯冲带是地球内外圈层碳交换的关键场所,每年通过俯冲作用进入地球内部的碳可达68~96 Mt(Plank and Manning,2019),可造成地幔同位素和挥发分组成不均一,是诱发地幔对流和深部岩浆活动的重要因素。据估算,自板片俯冲起始以来,通过俯冲带输运的碳远超过现今地表碳的总含量(2021—2030地球科学发展战略研究组,2021)。不同类型俯冲板片的脱碳效率差异较大,从最低约10%至高达100%,主要取决于板片自身的温度、流体活动性和碳的赋存方式等(Hirschmann,2018;Stewart and Ague,2020;Farsang et al.,2021)。平均而言,约25%~65%的二氧化碳可以通过流体溶解作用(Ague and Nicolescu,2014;Kelemen and Manning,2015;Farsang et al.,2021;Lan et al.,2023)、变质反应脱碳(Tao et al.,2018;Stewart and Ague,2020;Arzilli et al.,2023)或部分熔融作用(或含水碳酸盐流体)(Poli,2015;Thomson et al.,2016;Zhang et al.,2021,2023;Chen et al.,2023)等方式返回至地幔楔和大气中。从空间上看,弧前-弧下深度(~≤150 km)是俯冲板片大量脱碳的主要场所(Poli,2015;Stewart and Ague,2020;Arzilli et al.,2023),但并非所有的俯冲碳都会在该深度范围释放。在流体活动较弱或无流体活动的情况下,俯冲板片在弧前-弧下深度范围不会“完全脱碳”(Kerrick and Connolly,2001;Gorman et al.,2006;Tian et al.,2019),部分碳能够随俯冲板片一起进入上地幔底部或地幔过渡带,甚至下地幔(Harte et al.,1999;Walter et al.,2011;Thomson et al.,2014;Regier et al.,2020;Nestola et al.,2023;Zhang et al.,2024)。

考虑到俯冲板片的热状态差异,进入地幔深部的俯冲碳既可以通过部分熔融作用释放至周围地幔,也可能随俯冲板片一起进入深下地幔。进入周围地幔的含碳熔流体不仅能够通过熔岩反应和氧化还原反应把碳以金刚石的形式“冻结”在地幔深部,还可以通过多种途径(如岩浆活动、气体扩散)再次返回到地表或大气中(Rohrbach and Schmidt,2011;Kelemen and Manning,2015;Plank and Manning,2019)。比如:研究人员在中国东部多个地区的晚白垩世和新生代玄武岩和橄榄岩包体中发现了再循环碳酸盐的信息,这被认为是滞留在地幔过渡带的碳酸盐化洋壳或沉积物发生部分熔融并与地表岩浆活动相互联系的重要依据(Zhang et al.,2017;Wang et al.,2017;李曙光和汪洋,2018;徐义刚等,2018;宗克清和刘勇胜,2018;朱日祥和徐义刚,2019;Li et al.,2021;Liu et al.,2022;徐荣等,2022)。可见俯冲带深部碳循环不仅能影响深部地幔的物质组成、氧化还原状态和同位素特征(许成等,2017;张立飞等,2017;刘勇胜等,2019;Tao and Fei,2021),还与地表岩浆活动、大气CO_2浓度和地表温度变化密切相关(Müller et al.,2022;朱建江等,2022)。相对于大气或近地表碳循环,研究地球深部碳循环的方法比较有限,主要原因在于缺少直接观测手段和能获得的深部天然样品十分稀少。高温高压实验和理论计算是探索深部碳循环的正演手段,深源金刚石(来自软流圈或更深部地幔)是直接来自地幔深部的碳,包含了丰富的有关深部碳循环的重要信息,是探索深部碳循环的直接窗口。

1　深源金刚石分类和来源深度约束方法

金刚石主要由碳和极少量氮元素组成,一般认为金刚石的形成深度大于120 km(Kennedy and Kennedy,1976)。除此之外,金刚石自身并不能为我们提供更多有关形成深度的信息,因此制约金刚石的来源深度还需要依靠其矿物包裹体组合和包裹体的成分特征(Nimis,2022)。根据金刚石中主要矿物包裹体的种类和成分,可以把深源金刚石分为橄榄岩型金刚石和榴辉岩型金刚石,橄榄岩型金刚石可进一步分为富集橄榄岩型和亏损橄榄岩型(方辉橄榄岩型)(Walter et al.,2022;Shirey et al.,2024)。如表1所示,在上地幔和地幔过渡带,橄榄岩型金刚石中的矿物包裹体可能包括:橄榄石及其高压相、斜方辉石、单斜辉石或高压斜顽辉石、超硅石榴子石(高Cr)和毛钙硅石(低Ti);榴辉岩型金刚石中的矿物包裹体可能包括:超硅石榴子石(低Cr)、单斜辉石、斯石英和毛钙硅石(高Ti)。在下地幔顶部,橄榄岩型金刚石中的矿物包裹体可能包括:布里奇曼石(低Al)、铁方镁石和毛钙硅石;榴辉岩型金刚石中的矿物包裹体可能包括:超硅石榴子石(或CF-相、NAL-相)、斯石英、布里奇曼石(高Al)和和毛钙硅石。图1表示深源金刚石中典型的矿物包裹体,虽然金刚石中的矿物包裹体种类很多,但并非所有的矿物包裹体都能提供准确的深度信息,比如:橄榄石和斜方辉石在地表至上地幔底部均可以稳定存在,其化学成分与压力变化也没有明显的相关性,因此不具备提供准确深度信息的价值;同理,$CaSiO_3$包裹体(毛钙硅石成分)稳定的深度范围也比较宽(Woodland et al.,2020),且其形成机制比较复杂,因此能否用于指示金刚石来

表 1 不同类型金刚石及其主要矿物包裹体类型

Table 1 Types of major mineral inclusions in peridotitic- and eclogitic diamonds

类型/深度	上地幔(<410 km)	地幔过渡带(410~660 km)	下地幔(>660 km)
榴辉岩型金刚石	单斜辉石(高Na)、超硅石榴子石(低Cr)、柯石英/斯石英	超硅石榴子石(低Cr)、毛钙硅石(高Ti)、斯石英	超硅石榴子石(或CF-相、NAL-相)、布里奇曼石(高Al)、毛钙硅石(高Ti)、斯石英
橄榄岩型金刚石	橄榄石、斜方辉石、单斜辉石、超硅石榴子石(高Cr)	瓦兹利石或林伍德石、超硅石榴子石(高Cr)、毛钙硅石(低Ti)	布里奇曼石(低Al)、铁方镁石、毛钙硅石、(低Ti)

参考文献：Harte et al.,1999；Kaminsky et al.,2001；Harte,2010；Walter et al.,2011,2022；Kaminsky,2012；Thomson et al.,2014；Zedgenizov et al.,2014；Nestola et al.,2018；Tschauner et al.,2021；Stachel et al.,2022；Shirey et al.,2024。

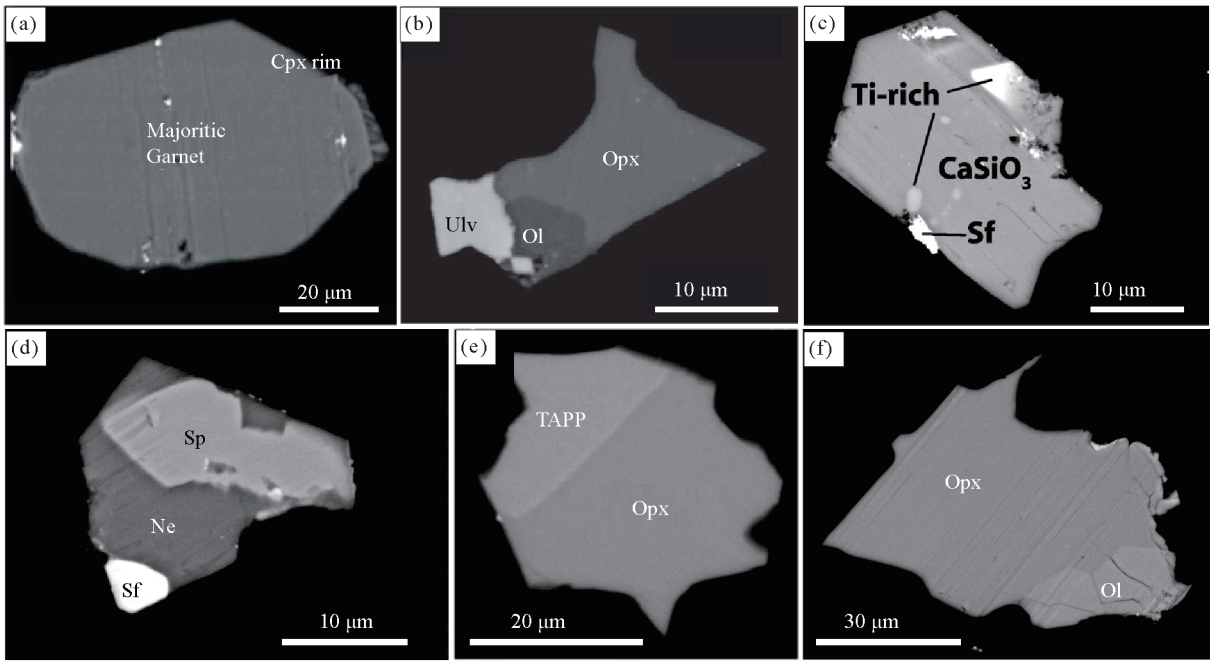

(a)有单斜辉石(Cpx)出溶边的超硅石榴子石包裹体(Bulanova et al.,2010)；(b)斜方辉石(Opx)、钛尖晶石(Ulv)和橄榄石(Ol)包裹体共存(Walter et al.,2011)；(c)$CaSiO_3$和硫化物(Sf)包裹体共存(Walter et al.,2011)；(d)霞石(Ne)、尖晶石(Sp)和硫化物(Sf)包裹体共存(Walter et al.,2011)；(e)斜方辉石(Opx)和四方晶系铁铝-镁铝榴石(TAPP)包裹体共存(Zedgenizov et al.,2014)；(f)斜方辉石(Opx)和橄榄石(Ol)包裹体共存(Burnham et al.,2016)

图1 深源金刚石中的典型矿物包裹体特征

Fig. 1 Backscattered electron images showing characteristics of typical mineral inclusions in deeply sourced diamonds

源深度仍存在争议(Walter et al.,2022)。常用于制约寄主金刚石来源深度的矿物包裹体包括：超硅石榴子石、橄榄石高压相(瓦兹利石和林伍德石)和石英高压相(柯石英和斯石英)等，以及各种矿物组合，比如：后尖晶石相和后石榴子石相矿物组合。由于橄榄石高压相(瓦兹利石和林伍德石)和石英高压相(柯石英和斯石英)包裹体比较少见，因此超硅石榴子石和各种矿物组合是最常用来约束金刚石起源深度的方法。除此之外，基于矿物包裹体残余压强建立的弹性-弹塑性压力计也被用于估算金刚石的形成深度(矿物包裹体的捕获深度)(Anzolini et al.,2019；Wang et al.,2021)。由于榴辉岩型深源金刚石的形成与俯冲洋壳脱碳相关(Walter et al.,2022)，其形成深度在一定程度上反应了深俯冲洋壳的脱碳深度，因此准确制约榴辉岩型金刚石的来源深度是认识俯冲带深部碳循迁移的关键。

2 榴辉岩型深源金刚石的来源深度

2.1 超硅石榴子石包裹体：软流圈和地幔过渡带金刚石的来源深度

超硅石榴子石是橄榄岩和榴辉岩体系的重要矿物之一，稳定范围从~150 km至地幔过渡带底部，其化学成分随深度增加而变化，因此可以根据超硅石榴子石包裹体的化学成分约束金刚石的最浅来源深度(Beyer and Frost,2017)。石榴子石的理论化学式为$A_3B_2Si_3O_{12}$，随着深度增加会发生如下两种主要替代机制，$2B^{3+}={}^{VI}M^{2+}+{}^{VI}Si^{4+}$[majorite]，$A^{2+}+B^{3+}={}^{VIII}X^{+}+{}^{VI}Si^{4+}$[Na-majorite]。由于橄榄岩和榴辉岩的全岩成分不同，因此橄榄岩和榴辉岩体系中形成的超硅石榴子石也具有不同的化学成分。根据

高温高压实验结果,橄榄岩型超硅石榴子石的主要替代机制为前者,榴辉岩型超硅石榴子石的主要替代机制为后者(Irifune et al.,1986;Irifune,1987)。因此可以根据超硅石榴子石包裹体的化学成分区分其形成环境。比如根据Cr含量不同,可以将超硅石榴子石包裹体划分为高Cr型(Cr_2O_3>1%)和低Cr型(Cr_2O_3<1%)两组。由于橄榄岩体系富Cr,该体系中形成的超硅石榴子石也相对富Cr,因此一般认为高Cr型超硅石榴子石形成于橄榄岩(方辉橄榄岩)体系,而低Cr型超硅石榴子石形成于榴辉岩体系(Bulanova et al.,2010;Harte,2010)。统计结果显示,大部分(~77%)含有超硅石榴子石包裹体的深源金刚石为榴辉岩型(或介于榴辉岩型和橄榄岩型之间),只有少部分(~23%)为橄榄岩型(Walter et al.,2022;Stachel et al.,2022)。

基于实验岩石学获得的超硅石榴子石压力计是估算超硅石榴子石及其寄主金刚石来源深度的重要依据(Beyer and Frost,2017;Thomson et al.,2021)。计算结果显示,大部分含有超硅石榴子石包裹体的深源金刚石形成于软流圈底部和地幔过渡带上部(图2)。其中,榴辉岩型深源金刚石有两个峰值,分别为~8~9 GPa和~14~15 GPa。橄榄岩型金刚石只有一个峰值,为~9~10 GPa。需要注意的是,超硅石榴子石包裹体在减压上升过程中可能会发生辉石出溶现象,从而导致计算得到的平衡压强偏低,因此要准确获得超硅石榴子石及其寄主金刚石的来源深度还需要考虑辉石出溶可能带来的影响。根据Thomson等(2021)的计算,辉石出溶可能会导致上述计算压强整体偏低~4 GPa。如果据此校正上述金刚石深度分布直方图,则大部分深源金刚石应该来源于地幔过渡带,仅有少量深源金刚石来源于软流圈底部。

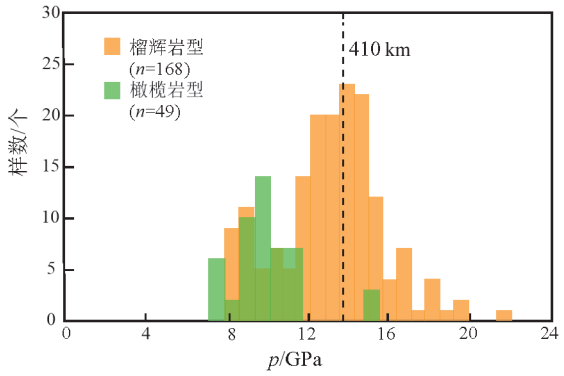

图2　含超硅石榴子石包裹体的深源金刚石深度分布图(修改自Shirey et al.,2024)

Fig. 2　Histogram for the distribution of depths of deeply sourced diamonds containing supersilicon garnet inclusions (modified after Shirey et al.,2024)

2.2　后尖晶石相和后石榴子石相矿物包裹体:下地幔金刚石的来源深度

在下地幔顶部(>660 km),林伍德石发生后尖晶石相变,分解为布里奇曼石($MgSiO_3$)和铁方镁石((Fe,Mg)O)。目前尚未发现具有布里奇曼石结构的$MgSiO_3$相包裹体,常见的$MgSiO_3$相包裹体具有顽火辉石或斜方辉石结构,因此当$MgSiO_3$相或(Fe,Mg)O相包裹体单独出现时,不能直接判断其形成深度。只有当$MgSiO_3$与(Fe,Mg)O包裹体共存时,可以认为是后尖晶石相矿物组合,来源深度大于660 km(McCammon,2001)。当深度为约680~720 km时,石榴子石逐渐分解为布里奇曼石和CF-相(富$NaAlSiO_4$),即后石榴子石相变。目前仅在巴西Juina-5金伯利岩的金刚石中发现了相对“完整”的后石榴子石相矿物组合,包括:$MgSiO_3$相、富$NaAlSiO_4$-相、富Al-相(NAL-相)和$CaSiO_3$相(Kaminsky et al.,2001;Walter et al.,2011;Thomson et al.,2014;Zedgenizov et al. 2014)。由于这些包裹体的化学成分与玄武岩体系中后石榴子石相矿物的化学成分基本一致,因此被认为是俯冲洋壳进入下地幔并返回地表的直接证据。

由于缺少有效的地质压力计,目前很难准确制约下地幔金刚石的来源深度。理论上,布里奇曼石的Al溶解度随压强升高而增加,因此在Al饱和的情况下可以根据布里奇曼石中的Al含量估算下地幔金刚石的来源深度(Hirose et al.,2001)。但实际情况中,通常很难发现$MgSiO_3$相包裹体与富Al矿物共存,也无法确定这些布里奇曼石包裹体是否Al饱和,从而限制了这种方法的应用。为了制约下地幔金刚石的来源深度,Shirey等(2021)将俯冲板片脱水脱碳和深源地震分布特征结合,通过假设俯冲板片释放的含碳酸盐流体诱发了深源地震,并根据深源地震的最大震源深度,推测下地幔榴辉岩型金刚石的形成深度可能不超过~800 km。由于很难证明碳酸盐流体活动与深源地震之间的因果关系,因此基于深源地震震源深度限定下地幔金刚石的形成深度存在很大不确定性。

2.3　$CaSiO_3$包裹体:能否指示金刚石来源深度

在洋壳和橄榄岩体系中,$CaSiO_3$相出现的压强为约20 GPa,具有钙钛矿结构,称为毛钙硅石(Tschauner et al.,2021)。一般情况下$CaSiO_3$相作为矿物包裹体单独出现,且不具备钙钛矿结构。特别是考虑到$CaSiO_3$相还可以通过其它机制形成,比如:$CaCO_3+SiO_2=CaSiO_3+CO_2$,因此仅根据$CaSiO_3$相包裹体无法准确判断寄主金刚石的来源深度。目前有2篇文献报道发现具有钙钛矿结构的$CaSiO_3$包裹体(Nestola et al.,2018;Tschauner et al.,2021),但结果存疑,比如:

Nestola等(2018)在南非Cullinan金刚石中发现$CaSiO_3$和$CaTiO_3$包裹体共生，XRD和EBSD分析结果显示$CaSiO_3$相具有钙钛矿结构，但这一结果与$CaSiO_3$-$CaTiO_3$相图矛盾，因为二者在高压下(>9 GPa)会形成固溶体，不能单独稳定存在(Kubo et al.，1997)，所以在利用$CaSiO_3$相包裹体指示金刚石来源深度时仍需要慎重。

3 俯冲洋壳脱碳与榴辉岩型深源金刚石的成因

3.1 俯冲洋壳脱碳过程的高温高压实验研究进展

俯冲洋壳是大洋板块的重要组成部分，主要由玄武岩、辉长岩和辉绿岩组成。在热液-海水交代作用和岩浆作用的影响下，蚀变洋壳中常含有一定量的二氧化碳，最高可达2.0%~5.0%(Kelley et al.，2003；Staudigel，2003)。据统计，俯冲洋壳中的碳含量约占俯冲带总碳输入量的20%~30%；当俯冲深度超过约150 km之后，洋壳中的碳含量约占俯冲板片残余总碳量的50%(Plank and Manning，2019；Müller et al.，2022)。可见俯冲洋壳在弧前-弧下的脱碳效率相对较低，具有把大量的碳输运至地幔深部的潜力。目前对俯冲含碳洋壳进行了大量高温高压实验研究(Yaxley and Green，1994；Molina and Poli，2000；Hammouda，2003；Yaxley and Brey，2004；Dasgupta et al.，2004；Poli et al.，2009；Litasov and Ohtani，2010；Keshav and Gudfinnsson，2010；Kiseeva et al.，2012，2013a；Poli，2015；Thomson et al.，2016；Martin and Hermann，2018；Elazar et al.，2019；Zhang et al.，2020，2023)和理论计算工作(Kerrick and Connolly，2001；Gorman et al.，2006；Tian et al.，2019；Menzel et al.，2020；Arzilli et al.，2023)，主要目的是确定俯冲洋壳的固相线(包括流体对固相线的影响)、碳酸盐矿物的赋存形式和脱碳效率等，以制约俯冲洋壳的脱碳过程。

图3总结了前人获得的俯冲含碳洋壳的固相线。总体而言，前人实验研究主要获得如下几点基本认识：(1)不同成分的碳酸盐化洋壳的固相线差异较大，影响固相线的主要因素包括H_2O、CO_2、Na_2O和K_2O的含量，以及Ca/Mg值等(Dasgupta et al.，2005)。(2)无水条件下，含碳洋壳在弧前-弧下深度的固相线高于典型俯冲带地温曲线，因此通常认为“干”俯冲洋壳在弧前-弧下不会发生部分熔融脱碳(Yaxley and Brey，2004；Dasgupta et al.，2004)。(3)无水条件下，典型变质反应脱碳所需要的温度条件均高于俯冲带地温曲线，因此“干”俯冲洋壳在弧前-弧下也不会发生变质反应脱碳(Luth，1995；Koziol and Newton，1995，1998)(图4)。(4)含水流体能够降低俯冲含碳洋壳的固相线，促使俯冲洋壳固相线与典型俯冲带地温曲线相交，导致俯冲洋壳发生部分熔融脱碳(深度>120~150 km)，这是热-暖俯冲洋壳重要的脱碳机制之一(Poli，2015；Martin and Hermann，2018；Zhang et al.，2023)。(5)在上地幔底部和地幔过渡带顶部，榴辉岩-石榴子石岩相变导致俯冲含碳洋壳的固相线由~1350 °C降低至~1150~1250 °C(Thomson et al.，2016；Zhang et al.，2020)，从而导致俯冲洋壳的固相线与热-暖俯冲带地温曲线相交，发生部分熔融脱碳；需要注意的是，Kiseeva 等(2013a)未发现榴辉岩-石榴子石岩相变伴随俯冲洋壳的固相线突降，推测这可能与他们的实验材料相对富K有关系，但还需要进一步验证。(6)使用简化体系来模拟俯冲洋壳的脱碳行为，能够降低实验的复杂性，但同时也可能带来一些问题：比如Litasov 和Ohtani(2010)和Keshav 和 Gudfinnsson (2010)分别对简化体系Na-CMAS+5% CO_2和CMAS +20% CO_2开展了高温高压实验研究，由于简化体系中不包含K(或Na)和Fe等元素，因而获得的固相线与复杂体系相比有较大区别(图3)，未必能够准确代表俯冲含碳洋壳的固相线。

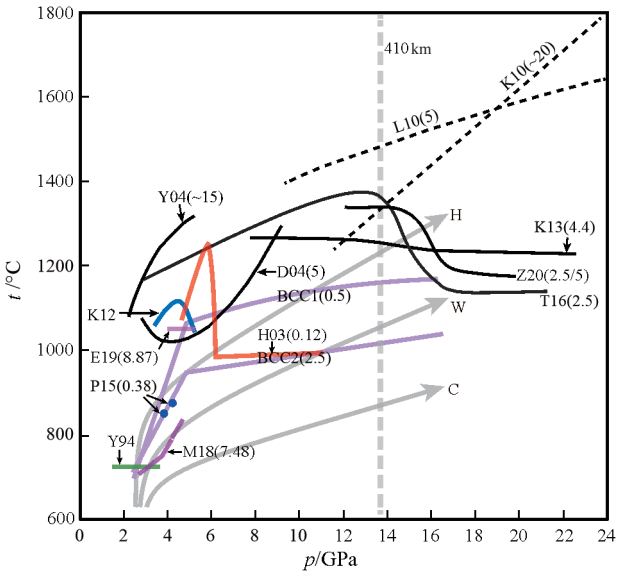

无水实验(括号中的数字表示二氧化碳含量)数据来源：D04(Dasgupta et al.，2004)；Y04(Yaxley and Brey，2004)；L10(Litasov and Ohtani，2010)；K10(Keshav and Gudfinnsson，2010)；K13(Kiseeva et al.，2013a)；T16(Thomson et al.，2016)；Z20(Zhang et al.，2020)。含水实验(括号中的数字表示水含量)数据来源：Y94(Yaxley and Green，1994)；H03(Hammouda，2003)；K12(Kiseeva et al.，2012)；P15(Poli，2015)；M18(Martin and Hermann，2018)；E19(Elazar et al.，2019)；Z23(Zhang et al.，2023)。俯冲带温度曲线(H—热；W—暖；C—冷)(Syracuse et al.，2010)

图3 俯冲含碳洋壳固相线与俯冲带地温曲线对比

Fig. 3 Comparison of the solidi curves of carbon-bearing oceanic crusts and typical geothermal curves of subduction zones

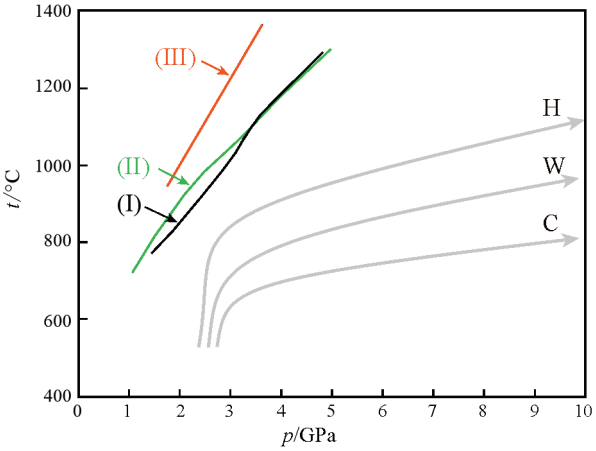

(I) $CaMg(CO_3)_2+2SiO_2=CaMgSi_2O_6+2CO_2$(Luth,1995);(II) $MgCO_3+SiO_2=MgSiO_3+CO_2$(Koziol and Newton,1995;Kakizawa et al.,2015);(III) $MgCO_3+MgSiO_3=Mg_2SiO_4+CO_2$(Koziol and Newton,1998)。俯冲带温度曲线(H—热;W—暖;C—冷)(Syracuse et al.,2010)

图4　典型变质反应脱碳条件与俯冲带地温曲线对比

Fig. 4　Comparison of P-T conditions of typical metamorphic decarbonation processes and geothermal curves of subduction zones

3.2　榴辉岩型深源金刚石的成因

从金刚石碳同位素的角度看,榴辉岩型金刚石的$\delta^{13}C$值介于–40.7‰~+2.5‰之间,其中约91%的数据集中在–20‰~0‰(图5a),特别是榴辉岩型深源金刚石的$\delta^{13}C$值几乎均小于0‰(图5b),这种碳同位素组成特征与蚀变洋壳具有很好的相似性(图5c),表明形成榴辉岩型金刚石的碳很可能来自俯冲蚀变洋壳(Li et al.,2019)。从金刚石内矿物包裹体的角度看,榴辉岩型金刚石中矿物包裹体的种类和成分与俯冲洋壳基本一致,再次表明其成因应该与俯冲洋壳脱碳密切相关(Walter et al.,2022)。实验研究发现,当俯冲含碳洋壳的固相线与俯冲带地温曲线相交时,首先形成低程度富钙碳酸盐熔体或含水碳酸盐熔体。在深度大于~250 km时,地幔的氧逸度主要受Fe-FeO反应控制,此时进入地幔的碳酸盐熔体与地幔橄榄岩发生氧化还原反应,导致部分碳以金刚石的形式被“冻结”下来(Frost and McCammon,2008;Rohrbach and Schmidt,2011;Kiseeva et al.,2013b,2018)。通过这种方式形成的金刚石不仅继承了蚀变洋壳的碳同位素特征,同时金刚石结晶过程中也极可能捕获洋壳矿物,因此可以称之为榴辉岩型金刚石。

图6a和6b对比了俯冲含碳洋壳的固相线剖面和基于超硅石榴子石压力计获得的榴辉岩型深源金刚石深度分布特征。在不考虑辉石出溶现象的情况下,大部分金刚石分布在软流圈底部和过渡带顶部,且具有两个明显的峰值。如果认为这些金刚石能够在一定程度上反映全部榴辉岩型金刚石的深度分布特征,则可

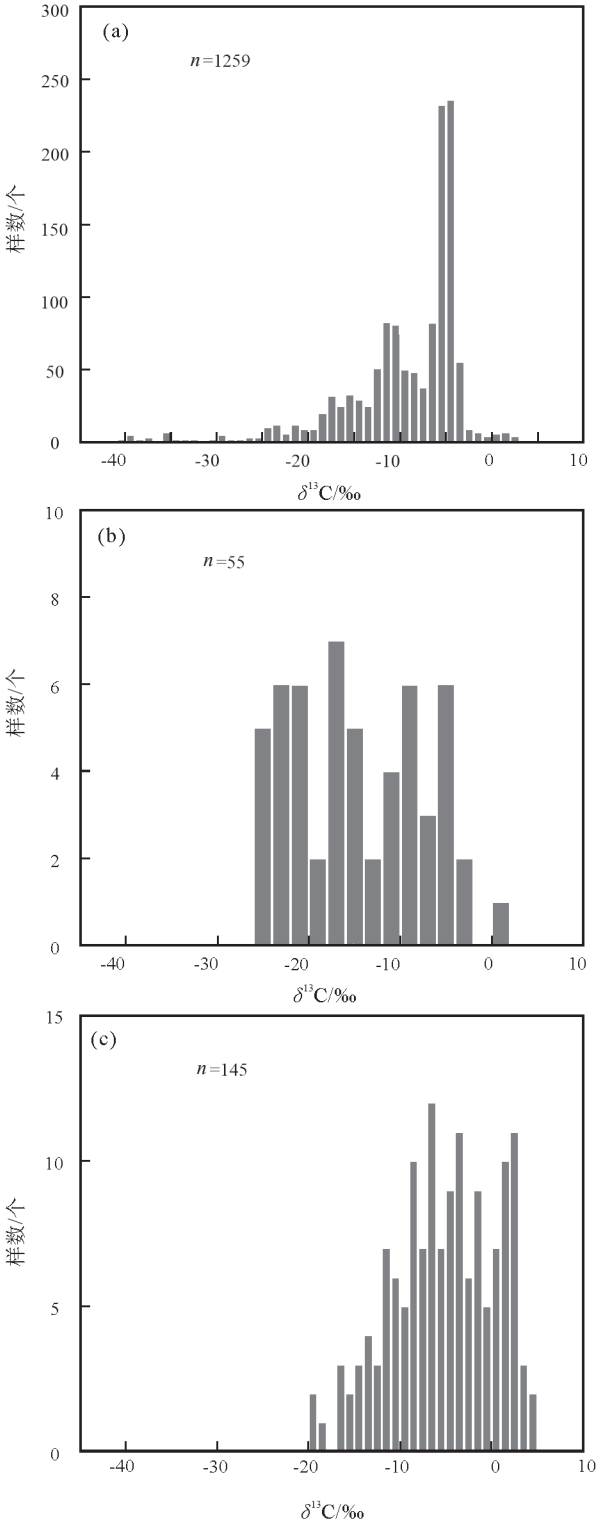

(a)所有榴辉岩型金刚石碳同位素数据;(b)深源(来源深度为软流圈或更深)榴辉岩型金刚石碳同位素数据;(c)蚀变洋壳碳同位素数据。榴辉岩型金刚石数据来自Stachel等(2022),蚀变洋壳数据来自Li 等(2019)

图5　榴辉岩型金刚石和蚀变洋壳碳同位素频率分布直方图

Fig.5　Histograms of $\delta^{13}C$ values of eclogitic diamonds and altered oceanic crusts

以对比讨论榴辉岩型金刚石的潜在成因机制。在上地幔范围内,“干”俯冲洋壳的固相线高于俯冲带地温

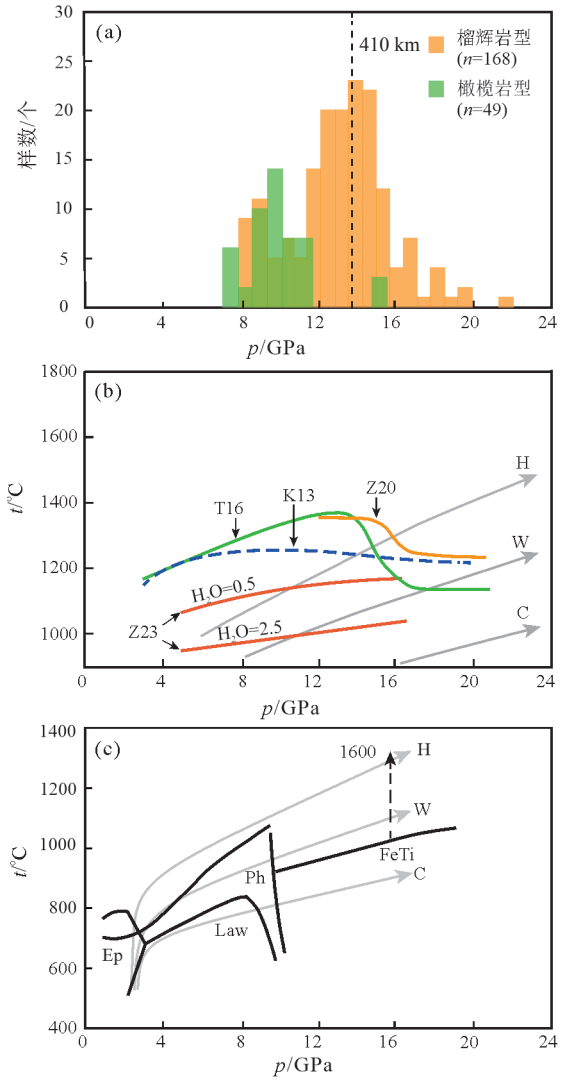

(a)修改自Shirey et al.,2024;(b)K13(Kiseeva et al.,2013a);T16(Thomson et al.,2016);Z20(Zhang et al.,2020);Z23(Zhang et al.,2023);(c)绿帘石(Ep)、硬柱石(Law)和多硅白云母(Ph)稳定范围参考Schmidt and Poli,2014,铁钛氢氧化物(FeTi)参考Nishihara and Matsukage,2016和Liu et al.,2019。俯冲带温度曲线(H—热;W—暖;C—冷)(Syracuse et al.,2010)。410 km指410 km地震不连续面

图6 含超硅石榴子石包裹体的金刚石深度分布图(a)与含碳洋壳固相线(b)和俯冲洋壳中含水矿物稳定范围(c)对比

Fig. 6 Comparisons of the distribution of depths of diamonds containg supersilicon garnet inclusions (a), the solidi curves of carbon-bearing oceanic crusts (b), and the stability of hydrous phases in subducted oceanic crusts (c)

曲线,因此“干”俯冲洋壳在上地幔不会发生部分熔融。只有流体存在的情况下含碳洋壳的固相线才可能与地温曲线相交,因此榴辉岩型金刚石在8~9 GPa深度附近的峰值极可能与水流体诱发的俯冲洋壳部分熔融脱碳有关系。基于俯冲洋壳中含水矿物稳定性(Schmidt and Poli,2014),硬柱石和多硅白云母最有可能在8~9 GPa附近脱水分解(图6c),从而为俯冲洋壳部分熔融脱碳提供水流体。据此可以推测,硬柱石或多硅白云母脱水分解诱发的部分熔融脱碳应该可以解释8~9 GPa深度附近榴辉岩型金刚石的成因。在14~15 GPa深度附近,榴辉岩-石榴子石岩相变导致俯冲含碳洋壳固相线突降,并与俯冲带地温曲线相交,从而促使洋壳发生低程度部分熔融,形成碳酸盐熔体。这些碳酸盐熔体与周围处于还原状态的地幔橄榄岩发生反应,可在地幔过渡带顶部形成大量金刚石。目前仅有少量关于超硅石榴子石包裹体和单斜辉石共存的数据报道(Thomson et al.,2021;Shirey et al.,2024),由于测试困难等原因很多文献未报道共存单斜辉石的化学成分。如果认为超硅石榴子石包裹体在减压上升过程中出溶辉石是一种普遍现象,则可以据此校正图6a中的金刚石深部分布直方图(Thomson et al.,2021)。这种情况下大部分超硅石榴子石的分布深度将位于地幔过渡带中部,此时榴辉岩型深源金刚石的成因更可能与榴辉岩-石榴子石岩相变导致的固相线突降相关,而与水流体诱发的部分熔融脱碳关系较弱。

4 问题与挑战

4.1 俯冲洋壳能否把大量碳输运至下地幔

对全球各地深源金刚石和超硅石榴子石包裹体的统计分析表明(Wang,1998;Walter et al.,2008;Kiseeva et al.,2013b,2018;Regier et al.,2020),大部分来自软流圈和地幔过渡带的金刚石具有俯冲洋壳和地幔橄榄岩的地球化学特征,这意味着俯冲洋壳不仅可以把大量的碳输运至地幔过渡带,而且能够在一定条件下发生部分熔融脱碳,富碳熔体与周围还原性的地幔橄榄岩反应,在形成金刚石的同时,也生成了具有玄武质洋壳和橄榄岩化学特征的超硅石榴子石包裹体。然而,统计结果发现大部分来自下地幔的金刚石(以及布里奇曼石和铁方镁石包裹体)缺少俯冲洋壳的地球化学信息(Cartigny et al.,2014;Regier et al.,2020;Meyer et al.,2023),这是否意味着俯冲洋壳难以将大量的碳输运至下地幔,亦或俯冲洋壳在下地幔顶部不会脱碳,还有待进一步研究。

4.2 下地幔榴辉岩型金刚石的来源深度

下地幔榴辉岩型金刚石包含了俯冲洋壳在下地幔的脱碳机制和碳迁移过程等重要信息,是探索下地幔碳循环的直接窗口。目前能够“确认”来自下地幔的榴辉岩型金刚石全部来自巴西Juina-5金伯利岩管(Kaminsky et al.,2001;Walter et al.,2011;Thomson et al.,2014),虽然数量十分稀少(8颗),但却明确显示深俯冲洋壳能够把部分碳输运至下地幔。Shirey等(2021)认为这些金

刚石的来源深度可能不超过~800 km,但他们的结论需要依赖很多假设,比如:含碳板片释放的碳酸盐流体诱发了深源地震和金刚石结晶。显然Shirey等(2021)推测的深源金刚石来源深度实际上代表深源地震的震源深度,能否真正代表深源金刚石的来源深度还需要更多证据。考虑到下地幔榴辉岩型金刚石直接指示了俯冲洋壳在下地幔的脱碳过程,因此有必要进一步研究下地幔榴辉岩型金刚石的普遍性及其来源深度。

4.3　(Fe, Mg)O包裹体的成因

(Fe,Mg)O相是深源金刚石中最常见的矿物包裹体之一,$Mg^{\#}$[$Mg^{\#}$=Mg/(Mg+Fe)]变化范围较大(0.15~0.95)(Kaminsky et al.,2001;Davies et al.,2003;Kaminsky,2012;Thomson et al.,2016)。在下地幔条件下,地幔橄榄岩(包括方辉橄榄岩)中形成的铁方镁石通常$Mg^{\#}$较高0.83~0.95。因此仅从$Mg^{\#}$的角度看,橄榄岩体系可以解释部分高$Mg^{\#}$(>0.83)(Fe,Mg)O包裹体的成因,但无法解释低$Mg^{\#}$(<0.83)(Fe,Mg)O的成因。有关低$Mg^{\#}$(Fe,Mg)O的成因有很多假设,比如:(1)来源于核幔边界或深下地幔(>1700 km)(Harte et al.,1999;Hayman et al.,2005);(2)下地幔范围内的连续脱碳反应(Liu,2002);(3)磁黄铁矿氧化与金刚石结晶(Jacob et al.,2016);(4)碳酸盐熔体与含铁地幔橄榄岩反应(Thomson et al.,2016),(5)复合铁氧化物的分解反应(Uenver-Thiele et al.,2017;Anzolini et al.,2020);(6)俯冲板片物质加入诱发的铁方镁石氧化反应(Kiseeva et al.,2022)。由于(Fe,Mg)O包裹体出现的频率远大于$MgSiO_3$包裹体,这与下地幔矿物组成比例不一致,且大部分情况下(Fe,Mg)O包裹体并不与$MgSiO_3$相共存,因此不能简单认为所有(Fe,Mg)O包裹体都是后尖晶石相变的产物或来自下地幔。特别是Anzolini等(2019)基于弹性-弹塑性理论发现金刚石中(Fe,Mg)O包裹体的捕获压力为~15 GPa,对应来源深度约为450 km。如果认为(Fe,Mg)O包裹体与寄主金刚石是同一过程或反应形成,则(Fe,Mg)O包裹体也可能是反应的产物,不一定与地幔橄榄岩体系的(Fe,Mg)O成分一致。Thomson等(2016)在地幔过渡带条件下开展了富钙碳酸盐熔体和橄榄岩反应的实验研究,发现该反应可以形成金刚石、镁方铁矿和石榴子石,其中石榴子石的成分与金刚石包裹体中发现的石榴子石包裹体基本一致,但镁方铁矿的$Mg^{\#}$很低(~0.2~0.4)。虽然从反应趋势看,该反应似乎能够解释低$Mg^{\#}$(Fe,Mg)O包裹体的成因,但是并没有形成$Mg^{\#}$为0.4~0.9的(Fe,Mg)O,不满足多数包裹体的成分特征。因此,(Fe,Mg)O包裹体的形成过程还需要进一步研究。

作者贡献声明: 张艳飞,论文构思、撰写和绘图;王超,论文构思;章军锋,论文构思和撰写;巫翔,论文构思;朱峰,论文构思。

利益冲突声明: 作者保证本文无利益冲突。

致谢: 评审专家提出的宝贵建议和意见对于提升本文有很大帮助,杂志编辑对本文进行了细致的校对工作,在此一并表示感谢。

参考文献 (References):

2021—2030地球科学发展战略研究组. 2021. 2021–2030地球科学发展战略——宜居地球的过去、现在与未来. 北京: 科学出版社. [Group of the Development Strategy of Earth Science 2021—2030. The past, present and future of the habitable Earth: Development strategy of Earth Science 2021–2030. Beijing: Science Press (in Chinese)]

Ague J J, Nicolescu S. 2014. Carbon dioxide released from subduction zones by fluid-mediated reactions. Nature Geoscience, 7: 355–360

Anzolini C, Nestola F, Mazzucchelli M L, Alvaro M, Nimis P, Gianese A, Morganti S, Marone F, Campione M, Hutchison M T, Harris J W. 2019. Depth of diamond formation obtained from single periclase inclusions. Geology, 47(3): 219–222

Anzolini C, Marquardt K, Stagno V, Bindi L C, Frost D J, Pearson D G, Harris J W, Hemley R J, Nestola F. 2020. Evidence for complex iron oxides in the deep mantle from FeNi(Cu) inclusions in superdeep diamond. Proceedings of the National Academy of Sciences of the United States of America, 117(35): 21088–21094

Arzilli F, Burton M, La Spina G, MacPherson C G, van Keken P E, McCann J. 2023. Decarbonation of subducting carbonate-bearing sediments and basalts of altered oceanic crust: Insights into recycling of CO_2 through volcanic arcs. Earth and Planetary Science Letters, 602: 117945

Beyer C, Frost D J. 2017. The depth of sub-lithospheric diamond formation and the redistribution of carbon in the deep mantle. Earth and Planetary Science Letters, 461: 30–39

Bulanova G P, Walter M J, Smith C B, Kohn S C, Armstrong L S, Blundy J, Gobbo L. 2010. Mineral inclusions in sublithospheric diamonds from Collier 4 kimberlite pipe, Juina, Brazil: subducted protoliths, carbonated melts and primary kimberlite magmatism. Contribution to Mineralogy and Petrology, 160: 489–510

Burnham A D, Bulanova G P, Smith C B, Whitehead S C, Kohn S C, Gobbo L, Walter M J. 2016. Diamonds from the Machado River alluvial deposit, Rondônia, Brazil, derived from both lithospheric and sublithospheric mantle. Lithos, 265: 199–213

Cartigny P, Palot M, Thomassot E, Harris J W. 2014. Diamond formation: A stable isotope perspective. Annual Review of Earth and Planetary Sciences, 42: 699–732

Chen W, Zhang G L, Keshav S, Li Y. 2023. Pervasive hydrous carbonatitic liquids mediate transfer of carbon from the slab to the subarc mantle. Communications Earth & Environment, 4: 73

Dasgupta R, Hirschmann M M, Withers A C. 2004. Deep global cycling of carbon constrained by the solidus of anhydrous, carbonated eclogite under upper mantle conditions. Earth and Planetary Science Letters, 227(1–2): 73–85

Dasgupta R, Hirschmann M M, Dellas N. 2005. The effect of bulk composition on the solidus of carbonated eclogite from partial melting experiments at 3GPa. Contributions to Mineralogy and Petrology, 149(3): 288–305

Davies R M, Griffin W L, O'Reilly S Y, Andrew A S. 2003. Unusual mineral inclusions and carbon isotopes of alluvial diamonds from Bingara, eastern Australia. Lithos, 69(1–2): 51–66

Elazar O, Frost D, Navon O, Kessel R. 2019. Melting of H_2O and CO_2-bearing eclogite at 4–6 GPa and 900–1200 ^oC: Implications for the generation of diamond-forming fluids. Geochimica et Cosmochica Acta, 255: 69–87

Farsang S, Louvel M, Zhao C S, Mezouar M, Rosa A D, Widmer R N, Feng X L, Liu J, Redfern S A T. 2021. Deep carbon cycle constrained by carbonate solubility. Nature Communications, 12(1): 4311

Frost D J, McCammon C A. 2008. The redox state of earth's mantle. Annual Review of Earth and Planetary Sciences, 36: 389–420

Gorman P J, Kerrick D M, Connolly J A D. 2006. Modeling open system metamorphic decarbonation of subducting slabs. Geochemistry, Geophysics, Geosystems, 7(4): Q04007

Hammouda T. 2003. High-pressure melting of carbonated eclogite and experimental constraints on carbon recycling and storage in the mantle. Earth and Planetary Science Letters, 214(1–2): 357–368

Harte B. 2010. Diamond formation in the deep mantle: the record of mineral inclusions and their distribution in relation to mantle dehydration zones. Mineralogical Magazine, 74(2): 189–215

Harte B, Harris J W, Hutchison M T, Watt G R, Wilding M C. 1999. Lower mantle mineral associations in diamonds from Sao Luiz, Brazil. In Mantle Petrology: Field Observations and High-Pressure Experimentation: A Tribute to Francis R.() Joe) Boyd. Editors: Fei Y W, Constance M. Bertka, Bjorn O. Mysen, pp. 125–153. Houston, TX: Geochem. Soc.

Hayman P C, Kopylova M G, Kaminsky F V. 2005. Lower mantle diamonds from Rio Soriso (Juina area, Mato Grosso, Brazil). Contributions to Mineralogy and Petrology, 149(4): 430–445

Hirose K, Fei Y W, Ono S, Yagi T, Funakoshi K I. 2001. *In situ* measurements of the phase transition boundary in $Mg_3Al_2Si_3O_{12}$: Implications for the nature of the seismic discontinuities in the Earth's mantle. Earth and Planetary Science Letters, 184(3–4): 567–573

Hirschmann M M. 2018. Comparative deep Earth volatile cycles: The case for C recycling from exosphere/mantle fractionation of major (H_2O, C, N) volatiles and from H_2O/Ce, CO_2/Ba, and CO_2/Nb exosphere ratios. Earth and Planetary Science Letters, 502: 262–273

Irifune T. 1987. An experimental investigation of the pyroxene-garnet transformation in a pyrolite composition and its bearing on the constitution of the mantle. Physics of the Earth and Planetary Interiors, 45(4): 324–336

Irifune T, Sekine T, Ringwood A E, Hibberson W O. 1986. The eclogite-garnetite transformation at high pressure and some geophysical implications. Earth and Planetary Science Letters, 77(2): 245–256

Jacob D E, Piazolo S, Schreiber A, Trimby P. 2016. Redox-freezing and nucleation of diamond via magnetite formation in the Earth's mantle. Nature Communications, 7: 11891

Kaminsky F. 2012. Mineralogy of the lower mantle: A review of 'super-deep' mineral inclusions in diamond. Earth Science Reviews, 110(1): 127–147

Kakizawa S, Inoue T, Suenami H, Kikegawa T. 2015. Decarbonation and melting in $MgCO_3$-SiO_2 system at high temperature and high pressure. Journal of Mineralogical and Petrological Sciences, 110: 179–188

Kaminsky F, Zakharchenko O, Davies R, Griffin W, Khachatryan-Blinova G, Shiryaev A. 2001. Superdeep diamonds from the Juina Area, Mato Grosso State, Brazil. Contributions to Mineralogy and Petrology, 140(6): 734–753

Kelley K A, Plank T, Ludden J, Staudigel H. 2003. Composition of altered oceanic crust at ODP Sites 801 and 1149. Geochemistry, Geophysics, Geosystems, 4(6): 8910

Kelemen P B, Manning C E. 2015. Reevaluating carbon fluxes in subduction zones, what goes down, mostly comes up. Proceedings of the National Academy of Sciences of the United States of America, 112(30): E3997–E4006

Kennedy C S, Kennedy G C. 1976. The equilibrium boundary between graphite and diamond. Journal of Geophysical Research, 81(14): 2467–2470

Kerrick D M, Connolly J A D. 2001. Metamorphic devolatilization of subducted oceanic metabasalts: Implications for seismicity, arc magmatism and volatile recycling. Earth and Planetary Science Letters, 189(1–2): 19–29

Keshav S, Gudfinnsson G H. 2010. Experimentally dictated stability of carbonated oceanic crust to moderately great depths in the Earth: Results from the solidus determination in the system CaO-MgO-Al_2O_3-SiO_2-CO_2. Journal of Geophysical Research: Solid Earth, 115(B5): B05205

Kiseeva E S, Yaxley G M, Hermann J, Litasov K D, Rosenthal A, Kamenetsky V S. 2012. An experimental study of carbonated eclogite at 3.5–5.5 GPa—Implications for silicate and carbonate metasomatism in the cratonic mantle. Journal of Petrology, 53(4): 727–759

Kiseeva E S, Litasov K D, Yaxley G M, Ohtani E, Kamenetsky V S. 2013a. Melting and phase relations of carbonated eclogite at 9–21 GPa and the petrogenesis of alkali-rich melts in the deep mantle. Journal of Petrology, 54(8): 1555–1583

Kiseeva E S, Yaxley G M, Stepanov A S, Tkalcic H, Litasov K D, Kamenetsky V S. 2013b. Metapyroxenite in the mantle transition zone revealed from majorite inclusions in diamonds. Geology, 41(8): 883–886

Kiseeva E S, Vasiukov D M, Wood B J, McCammon C, Stachel T, Bykov M, Bykova E, Chumakov A, Cerantola V, Harris J W, Dubrovinsky L. 2018. Oxidized iron in garnets from the mantle transition zone. Nature Geoscience, 11: 144–147

Kiseeva E S, Korolev N, Koemets I, Zedgenizov D A, Unitt R, McCammon C, Aslandukova A, Khandarkhaeva S, Fedotenko T, Glazyrin K, Bessas D, Aprilis G, Chumakov A I, Kagi H, Dubrovinsky L. 2022. Subduction-related oxidation of the sublithospheric mantle evidenced by ferropericlase and magnesiowüstite diamond inclusions. Nature Communications, 13: 7517

Koziol A M, Newton R C. 1995. Experimental determination of the reactions magnesite + quartz = enstatite + CO_2 and magnesite = periclase + CO_2, and enthalpies of formation of enstatite and magnesite. American Mineralogist, 80(11–12): 1252–1260

Koziol A M, Newton R C. 1998. Experimental determination of the reaction; magnesite + enstatite = forsterite + CO_2 in the ranges 6–25 kbar and 700–1100 degrees C. American Mineralogist, 83(3–4): 213–219

Kubo A, Suzuki T, Akaogi M. 1997. High pressure phase equilibria in the system $CaTiO_3$-$CaSiO_3$: stability of perovskite solid solutions. Physics and Chemistry of Minerals, 24: 488–494

Lan C Y, Tao R B, Huang F, Jiang R Z, Zhang L F. 2023. High-pressure experimental and thermodynamic constraints on the solubility of carbonates in subduction zone fluids. Earth and Planetary Science Letters, 603: 117989

李曙光, 汪洋. 2018. 中国东部大地幔楔形成时代和华北克拉通岩石圈减薄新机制: 深部再循环碳的地球动力学效应. 中国科学(地球科学), 48(7): 809–824［Li S G, Wang Y. 2018. Formation time of the big mantle wedge beneath Eastern China and a new lithospheric thinning mechanism of the North China Craton—Geodynamic effects of deep recycled carbon. Scientia Sinica(Terrae), 48(7): 809–824(in Chinese)］

Li K, Li L, Pearson D G, Stachel T. 2019. Diamond isotope compositions indicate altered igneous oceanic crust dominates deep carbon recycling. Earth and Planetary Science Letters, 516: 190–201

Li Y B, Weng A H, Xu W L, Zou Z L, Tang Y, Zhou Z K, Li S W, Zhang Y H, Ventura G. 2021. Translithospheric magma plumbing system of intraplate volcanoes as revealed by electrical resistivity imaging. Geology, 49(11): 1337–1342

刘勇胜, 陈春飞, 何德涛, 陈唯. 2019.俯冲带地球深部碳循环作用. 中国科学(地球科学), 49(12): 1982–2003［Liu Y S, Chen C F, He D T, Chen W. 2019.Deep carbon cycle in subduction zones. Scientia Sinica(Terrae), 49 (12): 1982–2003(in Chinese)］

Litasov K, Ohtani E. 2010. The solidus of carbonated eclogite in the system $CaO–Al_2O_3–MgO–SiO_2–Na_2O–CO_2$ to 32 GPa and carbonatite liquid in the deep mantle. Earth and Planetary Science Letters, 295(1–2): 115–126

Liu L G. 2002. An alternative interpretation of lower mantle mineral associations in diamonds. Contributions to Mineralogy and Petrology, 144 (1): 16–21

Liu S G, Qu Y R, Wang Z Z, Li M L, Yang C, Li S G. 2022. The fate of subducting carbon tracked by Mg and Zn isotopes: A review and new perspectives. Earth Science Reviews, 228: 104010

Liu X C, Matsukage K N, Nishihara Y, Suzuki T, Takahashi E. 2019. Stability of the hydrous phases of Al-rich phase D and Al-rich phase H in deep subducted oceanic crust. American Mineralogist, 104(1): 64–72

Luth R W. 1995. Experimental determination of the reaction dolomite + 2 coesite = diopside + 2 CO_2 to 6 GPa. Contributions to Mineralogy and Petrology, 122(1): 152–158

Martin L A J, Hermann J. 2018. Experimental phase relations in altered oceanic crust: Implications for carbon recycling at subduction zones. Journal of Petrology, 59(2): 299–320

McCammon C. 2001. Deep diamond mysteries. Science, 293(5531): 813–814

Menzel M D, Garrido C J, López Sánchez-Vizcaíno V. 2020. Fluid-mediated carbon release from serpentinite-hosted carbonates during dehydration of antigorite-serpentinite in subduction zones. Earth and Planetary Science Letters, 531: 115964

Meyer N A, Stachel T, Pearson D G, Stern R A, Harris J W, Walter M J. 2023. Diamonds reveal subducted slab harzburgite in the lower mantle. Geology, 51(3): 238–241

Molina J, Poli S. 2000. Carbonate stability and fluid composition in subducted oceanic crust: An experimental study on $H_2O–CO_2$-bearing basalts. Earth and Planetary Science Letters, 176(3–4): 295–310

Müller R D, Mather B, Dutkiewicz A, Keller T, Merdith A, Gonzalez C M, Gorczyk W, Zahirovic S. 2022. Evolution of Earth's tectonic carbon conveyor belt. Nature, 605(7911): 629–639

Nestola F, Regier M E, Luth R W, Pearson D G, Stachel T, McCammon C, Wenz M D, Jacobsen S D, Anzolini C, Bindi L C, Harris J W. 2023. Extreme redox variations in a superdeep diamond from a subducted slab. Nature, 613(7942): 85–89

Nestola F, Korolev N, Kopylova M, Rotiroti N, Pearson D G, Pamato M G, Alvaro M, Peruzzo L, Gurney J J, Moore A E, Davidson J. 2018. $CaSiO_3$ perovskite in diamond indicates the recycling of oceanic crust into the lower mantle. Nature, 555: 237–241

Nimis P. 2022. Pressure and Temperature date for diamonds. Reviews in Mineralogy & Geochemistry, 88: 533–566

Nishihara Y, Matsukage K N. 2016. Iron-titanium oxyhydroxides as water carriers in the Earth's deep mantle. American Mineralogist, 101(4): 919–927

Plank T, Manning C E. 2019. Subducting carbon. Nature, 574(7778): 343–352

Poli S. 2015. Carbon mobilized at shallow depths in subduction zones by carbonatitic liquids. Nature Geoscience, 8: 633–636

Poli S, Franzolin E, Fumagalli P, Crottini A. 2009. The transport of carbon and hydrogen in subducted oceanic crust: An experimental study to 5 GPa. Earth and Planetary Science Letters, 278(3–4): 350–360

Regier M E, Pearson D G, Stachel T, Luth R W, Stern R A, Harris J W. 2020. The lithospheric-to-lower-mantle carbon cycle recorded in superdeep diamonds. Nature, 585(7824): 234–238

Rohrbach A, Schmidt M W. 2011. Redox freezing and melting in the Earth's deep mantle resulting from carbon-iron redox coupling. Nature, 472 (7342): 209–212

Schmidt M W, Poli S. 2014. Devolatilization during subduction. In: Treatise on Geochemistry. Amsterdam: Elsevier: 669–701

Shirey S B, Wagner L S, Walter M J, Pearson D G, van Keken P E. 2021. Slab transport of fluids to deep focus earthquake depths—Thermal modeling constraints and evidence from diamonds. AGU Advances, 2(2): e2020AV000304

Shirey S B, Pearson D G, Stachel T, Walter M J. 2024. Sublithospheric diamonds: Plate tectonics from earth's deepest mantle samples. Annual Review of Earth and Planetary Sciences, 52: 249–293

Stachel T, Aulbach S, Harris J W. 2022. Mineral inclusions in lithospheric diamonds. Reviews in Mineralogy and Geochemistry, 88(1): 307–391

Stachel T, Cartigny P, Chacko T, Pearson D G. 2022. Carbon and nitrogen in mantle-derived diamonds. Reviews in Mineralogy and Geochemistry, 88 (1): 809–875

Staudigel H. 2003. Hydrothermal alteration processes in the oceanic crust. Treatise on Geochemistry, 3: 659

Stewart E M, Ague J J. 2020. Pervasive subduction zone devolatilization recycles CO_2 into the forearc. Nature Communications, 11: 6220

Syracuse E M, van Keken P E, Abers G A. 2010. The global range of subduction zone thermal models. Physics of the Earth and Planetary Interiors, 183(1–2): 73–90

Tao R B, Fei Y W. 2021. Recycled calcium carbonate is an efficient oxidation agent under deep upper mantle conditions. Communications Earth & Environment, 2: 45

Tao R B, Zhang L F, Tian M, Zhu J J, Liu X, Liu J Z, Höfer H E, Stagno V, Fei Y W. 2018. Formation of abiotic hydrocarbon from reduction of carbonate in subduction zones: Constraints from petrological observation and experimental simulation. Geochimica et Cosmochimica Acta, 239: 390–408

Thomson A R, Kohn S C, Bulanova G P, Smith C B, Araujo D, Walter M J, EIMF. 2014. Origin of sub-lithospheric diamonds from the Juina-5 kimberlite (Brazil): Constraints from carbon isotopes and inclusion compositions. Contributions to Mineralogy and Petrology, 168(6): 1081

Thomson A R, Walter M J, Kohn S C, Brooker R A. 2016. Slab melting as a barrier to deep carbon subduction. Nature, 529(7584): 76–79

Thomson A R, Kohn S C, Prabhu A, Walter M J. 2021. Evaluating the formation pressure of diamond hosted majoritic garnets: A machine learning majorite barometer. Journal of Geophysical Research (Solid Earth), 126(3): e2020JB020604

Tian M, Katz R F, Rees Jones D W, May D A. 2019. Devolatilization of subducting slabs, part II: Volatile fluxes and storage. Geochemistry, Geophysics, Geosystems, 20(12): 6199–6222

Tschauner O, Huang S C, Yang S Y, Humayun M, Liu W J, Gilbert Corder S N, Bechtel H A, Tischler J, Rossman G R. 2021. Discovery of davemaoite, $CaSiO_3$-perovskite, as a mineral from the lower mantle. Science, 374(6569): 891–894

Uenver-Thiele L, Woodland A B, Ballaran T B, Miyajima N, Frost D J. 2017. Phase relations of Fe-Mg spinels including new high-pressure post-spinel phases and implications for natural samples. American Mineralogist, 102 (10): 2054–2064

Walter M J, Bulanova G P, Armstrong L S, Keshav S, Blundy J D, Gudfinnsson G, Lord O T, Lennie A R, Clark S M, Smith C B, Gobbo L. 2008. Primary carbonatite melt from deeply subducted oceanic crust. Nature, 454(7204): 622–625

Walter M J, Kohn S C, Araujo D, Bulanova G P, Smith C B, Gaillou E, Wang J, Steele A, Shirey S B. 2011. Deep mantle cycling of oceanic crust: Evidence from diamonds and their mineral inclusions. Science, 334 (6052): 54–57

Walter M J, Thomson A R, Smith E M. 2022. Geochemistry of silicate and oxide inclusions in sublithospheric diamonds. Reviews in Mineralogy and Geochemistry, 88(1): 393–450

Wang W Y. 1998. Formation of diamond with mineral inclusions of "mixed" eclogite and peridotite paragenesis. Earth and Planetary Science Letters, 160(3–4): 831–843

Wang W Z, Tschauner O, Huang S C, Wu Z Q, Meng Y F, Bechtel H, Mao H K. 2021. Coupled deep-mantle carbon-water cycle: Evidence from lower-mantle diamonds. Innovation(Cambridge Mass), 2(2): 100117

Wang X J, Chen L H, Hofmann A W, Mao F G, Liu J Q, Zhong Y, Xie L W, Yang Y H. 2017. Mantle transition zone-derived EM1 component beneath NE China: Geochemical evidence from Cenozoic potassic basalts. Earth and Planetary Science Letters, 465: 16–28

Woodland A B, Girnis A V, Bulatov V K, Brey G P, Hofer H E. 2020. European Journal of Mineralogy, 32(1): 171–185

许成, 曾亮, 宋文磊, 冯梦, 邓淼, 韦春婉. 2017. 造山带碳酸岩起源与深部碳循环. 矿物岩石地球化学通报, 36(2): 213–221［Xu C, Zeng L, Song W L, Feng M, Deng M, Wei C W. 2017. Orogenic carbonatite petrogenesis and deep carbon recycle. Bulletin of Mineralogy, Petrology and Geochemistry, 36(2): 213–221(in Chinese)］

徐荣, 刘勇胜, 张艳飞, 邹宗琪, 张军波. 2022. 碳酸盐化榴辉岩对板内碱性玄武岩源区的贡献. 岩石学报, 38(12), 3771–3784［Xu R, Liu Y S, Zhang Y F, Zou Z Q, Zhang J B. 2022. Carbonated eclogite in the mantle source of intraplate alkaline basalts. Acta Petrologica Sinica, 38(12): 3771–3784(in Chinese)］

徐义刚, 李洪颜, 洪路兵, 马亮, 马强, 孙明道. 2018. 东亚大地幔楔与中国东部新生代板内玄武岩成因. 中国科学(地球科学), 48(7): 825–843［Xu Y G, Li H Y, Hong L B, Ma L, Ma Q, Sun M D. 2018. Generation of Cenozoic intraplate basalts in the big mantle wedge under eastern Asia. Scientia Sinica()Terrae), 48(7): 825–843(in Chinese)］

Yaxley G M, Brey G P. 2004. Phase relations of carbonate-bearing eclogite assemblages from 2.5 to 5.5GPa: Implications for petrogenesis of carbonatites. Contributions to Mineralogy and Petrology, 146(5): 606–619

Yaxley G M, Green D H. 1994. Experimental demonstration of refractory carbonate-bearing eclogite and siliceous melt in the subduction regime. Earth and Planetary Science Letters, 128(3–4): 313–325

Zedgenizov D A, Kagi H, Shatsky V S, Ragozin A L. 2014. Local variations of carbon isotope composition in diamonds from São-Luis()Brazil): Evidence for heterogenous carbon reservoir in sublithospheric mantle. Chemical Geology, 363: 114–124

Zhang G L, Chen L H, Jackson M G, Hofmann A W. 2017. Evolution of carbonated melt to alkali basalt in the South China Sea. Nature Geoscience, 10: 229–235

张立飞, 陶仁彪, 朱建江. 2017.俯冲带深部碳循环: 问题与探讨. 矿物岩石地球化学通报, 36(2): 185–196［Zhang L F, Tao R B, Zhu J J. 2017. Some problems of deep carbon cycle in subduction zone. Bulletin of Mineralogy, Petrology and Geochemistry, 36(2): 185–196(in Chinese)］

Zhang Q W, Timmerman S, Stachel T, Chinn I, Stern R A, Davies J, Nestola F, Luth R, Pearson D G. 2024. Sublithospheric diamonds extend Paleoproterozoic record of cold deep subduction into the lower mantle. Earth and Planetary Science Letters, 634: 118675

Zhang Y F, Wang C, Jin Z M. 2020. Decarbonation of stagnant slab in the mantle transition zone. Journal of Geophysical Research: Solid Earth, 125 (7): e2020JB019533

Zhang Y F, Xu Q J, Wang C, Jin Z M. 2021. Release of CO_2 in cold subduction zones by hydrous carbonatitic liquids. Geophysical Research Letters, 48 (7): e2021GL092550

Zhang Y F, Wang C, Li W, Jin Z M. 2023. Carbon dioxide released from subducted oceanic crust by hydrous carbonatitic liquids. Geophysical Research Letters, 50(18): e2023GL104734

朱建江, 刘福来, 张立飞. 2022. 地球早期碳循环与大氧化事件. 岩石矿物学杂志, 41(2): 396–412［Zhu J J, Liu F L, Zhang L F. 2022. Carbon cycle in the early Earth and the great oxidation even. Acta Petrologica et Mineralogica, 41(2): 396–412(in Chinese)］

朱日祥, 徐义刚. 2019.西太平洋板块俯冲与华北克拉通破坏. 中国科学(地球科学), 49(9): 1346–1356［Zhu R X, Xu Y G. 2019.The subduction of the Western Pacific plate and the destruction of the North China Craton. Scientia Sinica(Terrae), 49(9): 1346–1356(in Chinese)］

宗克清, 刘勇胜. 2018.华北克拉通东部岩石圈地幔碳酸盐熔体交代作用与克拉通破坏. 中国科学(地球科学), 48(6): 732–752［Zong K Q, Liu Y S. 2018.Carbonate metasomatism in the lithospheric mantle: Implications for cratonic destruction in North China. Scientia Sinica(Terrae), 48(6): 732–752(in Chinese)］

（本文责任编辑：龚超颖；英文审校：张兴春）